MedCrave
Step into the World of Research

Journal of Nanomedicine Research

Review Article

Open Access

CrossMark

DNA compaction and particle formation by synthetic polymers: applications in gene delivery

Abstract

We have reviewed the effects of synthetic polymers on DNA compaction and particle formation. Synthetic polymers such as poly (ethylene glycol) PEG-(PEG-3350, PEG-6000), methoxypoly (ethylene glycol) anthracene (mPEG-anthracene), methoxypoly (ethylene glycol) poly (amidoamine) (mPEG-PAMAM-G3), (mPEG-PAMAM-G4) and poly(amidoamine) (PAMAM-G4) alter DNA structure and dynamic. The spectroscopic results and atomic force microscopic (AFM) were analysed and the effect of synthetic polymer complexation on DNA stability, aggregation, compaction and particle formation are discussed. A comparison of the overall binding constants showed that the order of binding PAMAM-G4>PEG-6000>PEG-3350>mPEG-anthracene> mPEG-PAMAM-G4>mPEG-PAMAM-G3. The morphology and ultrastructure of polymer-DNA adducts showed major DNA compaction and particle formation induced by synthetic polymers. The generated information is useful for the application of synthetic nanoparticles in gene delivery.

Keywords: PEG, Dendrimer, DNA, Particle formation, Spectroscopy, AFM

Volume 2 Issue 4 - 2015

Froehlich E,[1] Mandeville JS,[1] Bekale L,[1] Kreplak L,[2] Tajmir-Riahi HA[1]

[1]Department of Chemistry-Physics, University of Quebec at Trois-Rivieres, Canada

[2]Department of Physics, Dalhousie University, Canada

Correspondence: Tajmir-Riahi HA, Department of Chemistry-Physics, University of Quebec at Trois-Rivieres, C.P.500, Trois-Rivieres (Quebec), G9A 5H7, Canada, Tel 819-376-5011 (Ext. 3310, Fax 819-376-5084 Email tajmirri@uqtr.ca

Received: October 21, 2015 | **Published:** November 30, 2015

Abbreviations: PEG, Poly(Ethylene Glycol); mPEG, Methoxypoly (Ethylene Glycol); PAMAM, Poly(Amidoamine); CD, Circular Dichroism; FTIR, Fourier Transform Infrared; AFM, Atomic Force Microscopy

Introduction

Synthetic polymers of a specific shape and size are widely used as drug and gene delivery tools in pharmaceutical and nanomedicine biotechnology.[1,2] Poly (ethylene glycol) and its derivatives show major applications in gene and drug delivery due to their solubility, nontoxicity and biocompatibility.[3-6] Dendrimers, a family of cationic polymers, are promising nonviral tools for gene and drug delivery because of a well-defined molecular shape, controlled chemical structure, high water solubility, large number of chemically versatile surface groups, and unique architecture.[7-14] It has been shown that synthetic polymers induce significant changes in DNA solubility and structure under given conditions. PEGylation of synthetic polymers such as dendrimers is shown to reduce toxicity and increase biocompatibility and DNA transfection.[15-21] It is well demonstrated that synthetic polymers induce DNA aggregation and particle formation.[21-25] Therefore, it was of interest to review and compare the effects of several synthetic polymers on DNA compaction and particle formation that are recently reported.[22-24]

Here, we compare the bindings of DNA to several synthetic polymers such as PEG-3350, PEG-6000 and mPEG-anthracene, mPEG-PAMA-G3, mPEG-PAMAM-G4 and PAMAM-G4 at physiological conditions. The data obtained from multiple spectroscopic measurements and AFM microscopic images will be analysed and the effects of various synthetic polymers on DNA compaction and particle formation are discussed here.

Experimental

Atomic force microscopy: Polymer-DNA complexes at a ratio of 1:1 and final DNA concentration of 0.1 mM were prepared in 5 ml Tris-HCl (pH 7.4). The solutions were either used undiluted or diluted further in ultrapure water. For each sample, 30 µl aliquot was adsorbed for two minutes on freshly cleaved muscovite mica. The surface was rinsed thoroughly with 10 ml of ultrapure water and dried with Argon. AFM imaging was performed in acoustic mode at a scanning speed of 1Hz with an Agilent 5500 (Agilent, Santa Barbara, CA) using high frequency (300 kHz) silicon cantilevers with a tip radius of 2-5 nm (TESP-SS, Veeco, Santa Barbara, CA).[26] Images were treated using the software Gwyddion (http://gwyddion.net/).

FTIR spectroscopy: Infrared spectra were recorded on a FTIR spectrometer (Impact 420 model), equipped with DTGS (deuterated triglycine sulfate) detector and KBr beam splitter, using AgBr windows. Spectra were collected after 2h incubation of polymer with the DNA solution and measured. Interferograms were accumulated over the spectral range 4000-600 cm^{-1} with a nominal resolution of 2 cm^{-1} and a minimum of 100 scans. The difference spectra [(DNA solution + polymer) - (DNA solution)] were obtained, using a sharp band at 968 (DNA) as internal reference. This band, which is due to sugar C-C stretching vibrations, exhibits no spectral changes (shifting or intensity variations) upon polymer-polynucleotide complexation, and cancelled out upon spectral subtraction.[26]

CD spectroscopy: The CD spectra of DNA and its polymer adducts were recorded at pH 7.3 with a Jasco J-720 spectropolarimeter. For measurements in the Far-UV region (200-320 nm), a quartz cell with a path length of 0.01 cm was used. Six scans were accumulated at a scan speed of 50 nm per minute, with data being collected at every nm from 200 to 320 nm. Sample temperature was maintained at 25 °C using a Neslab RTE-111 circulating water bath connected to the water-jacketed quartz cuvette. Spectra were corrected for buffer signal and conversion to the Mol CD (Δε) was performed with the Jasco Standard Analysis software.[26]

UV absorption spectroscopy: The absorption spectra were recorded on a Perkin Elmer Lambda 40 Spectrophotometer with a slit of 2 nm and scan speed of 240 nm min^{-1}. Quartz cuvettes of 1 cm were used. The absorbance assessments were performed at pH 7.3 by keeping the concentration of DNA constant (125 µM), while varying polymer contents (5 to 100 µM). The binding constants of polymer-DNA adducts were calculated as reported.[26]

It is assumed that the interaction between the ligand L and the substrate S is 1:1; for this reason a single complex SL (1:1) is formed. It was also assumed that the sites (and all the binding sites) are independent and finally the Beer's law is followed by all species. A wavelength is selected at which the molar absorptivities ε_S (molar absorptivity of the substrate) and ε_{11} (molar absorptivity of the complex) are different. Then at total concentration S_t of the substrate, in the absence of ligand and the light path length is b = 1 cm, the solution absorbance is:

$$A_0 = \varepsilon_s b S_t \qquad (1)$$

In the presence of ligand at total concentration L_t, the absorbance of a solution containing the same total substrate concentration is:

$$A_L = \varepsilon_s b[S] + \varepsilon_L b[L] + \varepsilon_{11} b[SL] \quad (2)$$

(where [S] is the concentration of the uncomplexed substrate, [L] the concentration of the uncomplexed ligand and [SL] is the concentration of the complex) which, combined with the mass balance on S and L, gives:

$$A_L = \varepsilon_s b S_t + \varepsilon_L b L_t + \Delta\varepsilon_{11} b[SL] \quad (3)$$

where $\Delta\varepsilon_{11} = \varepsilon_{11} - \varepsilon_S - \varepsilon_L$ (ε_L molar absorptivity of the ligand). By measuring the solution absorbance against a reference containing ligand at the same total concentration L_t, the measured absorbance becomes:

$$A = \varepsilon_s b S_t + \Delta\varepsilon_{11} b[SL] \qquad (4)$$

Combining equation (4) with the stability constant definition $K_{11} = [SL]/[S][L]$, gives:

$$\Delta A = K_{11}\Delta\varepsilon_{11} b[S][L] \qquad (5)$$

where $\Delta A = A - A_o$. From the mass balance expression $S_t = [S] + [SL]$ we get $[S] = S_t/(1 + K_{11}[L])$, which is equation (5), giving equation (6) at the relationship between the observed absorbance change per centimeter and the system variables and parameters.

$$\frac{\Delta A}{b} = \frac{S_t K_{11}\Delta\varepsilon_{11}[L]}{1 + K_{11}[L]} \qquad (6)$$

Equation (6) is the binding isotherm, which shows the hyperbolic dependence on free ligand concentration.

The double-reciprocal form of plotting the rectangular hyperbola $\frac{1}{y} = \frac{f}{d}.\frac{1}{x} + \frac{e}{d}$ is based on the linearization of equation (6) according to the following equation:

$$\frac{b}{\Delta A} = \frac{1}{S_t K_{11}\Delta\varepsilon_{11}[L]} + \frac{1}{S_t\Delta\varepsilon_{11}} \qquad (7)$$

Thus the double reciprocal plot of 1/ΔA versus 1/[L] is linear and the binding constant can be estimated from the following equation:

$$K_{11} = \frac{intercept}{slope} \qquad (8)$$

Fluorescence spectroscopy: Fluorometric experiments were carried out on a Varian Cary Eclipse. Solution of mPEG-anthracene (80 μM) was prepared at 25 ±1 °C. Various solutions of DNA (5 to 100 μM) in 10 mM Tris-HCl (pH 7.4) were also prepared at 25 ±1 °C. The fluorescence spectra were recorded at λ_{exc} = 300-350 nm and λ_{em} 400-450 nm. The intensity variations at 420 nm was used to calculate the binding constant (K) for mPEG-anthracene-DNA adducts.

Discussion

Ultrastructure of polymer-DNA adducts by AFM images

DNA compaction, condensation and particle formation were observed in the presence of PEG, mPEG-anthracene, dendrimers and PEGylated dendrimers (Figure 1). PEG-3350 and PEG-6000 sample showed clear evidence of complexation by AFM images (Figure 1 Panel A). However, this was not the case for the mPEG-Anthracene sample where naked DNA strands could be observed on the mica surface (Figure 1, panel A & C). For the PEG 3350 sample, the complexation was not complete with the presence of DNA strands with a beaded appearance (Figure 1 Panel A). For the PEG 6000 sample, the complexation was much more extensive. The surface was covered with "fried-egg" aggregates similar to the ones observed previously for DOTAP-DNA mixtures.[26] The PEG 6000 complexes had an average height of 7.4 (0.2 nm (n =904) and an average volume of 390000 ± 6600 nm^3 (n = 904).

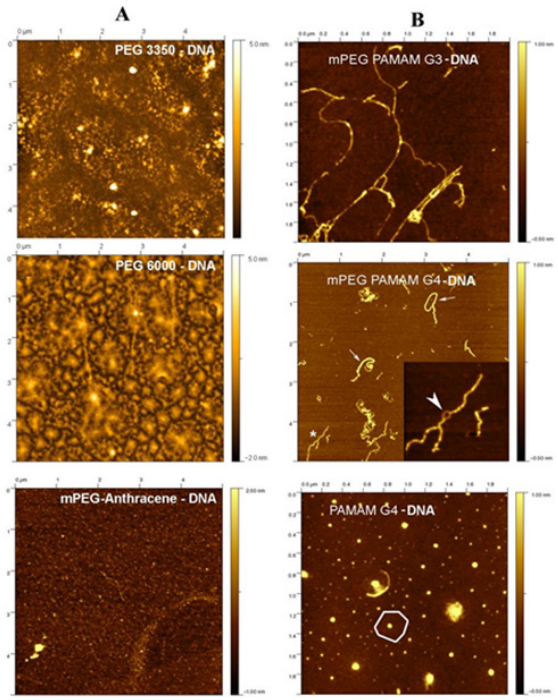

Figure 1 Tapping mode AFM images in air of synthetic polymer-DNA complexes diluted 10 or 100 times in ultrapure water and adsorbed to mica. In all three cases, the surface was covered with aggregates.

Panel A: complexes with PEG 3350, PEG 6000 and mPEG-anthracene and

Panel B: for complexes with mPEG-PAMAM-G3, mPEG-PAMAM-G4 and PAMAM-G4.

The AFM images reveal two different types of interactions between the dendrimers and DNA molecules (Figure 1, panel B). The two mPEG terminated dendrimers tend to coat and bundle DNA molecules (Figure 1, panel B). In the case of mPEG-PAMAM-G4, ring-like structures were observed along some of the bundles (Figure 1, panel B) that can be attributed to two "naked" DNA molecules repelling each other (Figure 1, panel B). In contrast, PAMAM-G4 was able to compact DNA into aggregates exhibiting a central core surrounded by a flat region (Figure 1, panel B). These complexes were similar to those observed for a mixture of positively charged lipid (DOTAP) and DNA, in a previous study.[26] The condensation and compaction

Citation: Froehlich E, Mandeville JS, Bekale L, et al. DNA compaction and particle formation by synthetic polymers: applications in gene delivery. *J Nanomed Res.* 2015;2(4):117–122. DOI: 10.15406/jnmr.2015.02.00038

of DNA by dendrimers was observed, particularly with PAMAM-G4 (Figure 1, panel B). It is well demonstrated that dendrimers induce DNA compaction and particle formation.[22,24]

Binding process of synthetic polymers to DNA duplex

Synthetic polymer complexes with DNA *via* hydrophilic, hydrophobic contacts, groove binding and phosphate interaction.[27-31] The infrared spectra and difference spectra of the free DNA showed major alterations of DNA in-plane vibrations at 1710 (guanine), 1661 (thymine), 1610 (adenine) and the backbone phosphate at 1225 asymmetric (PO_2) and 1088 cm^{-1} symmetric (PO_2) stretching bands.[27-31] upon polymer complexation (Figure 2, panels A&B). Low concentration (0.125 mM) of synthetic polymers PEG-3350, PEG-6000, mPEG-PAMAM-G3, mPEG-PAMAM-G4 and PAMAM-G4 induced minor changes of DNA vibrational frequencies, while at high polymer content (1 mM) major alterations of DNA in-plane and the backbone vibrational frequencies (Figure 2, panels A&B). The major intensity increases were associated with the guanine at 1710 (guanine N7), thymine at 1661 (thymine O_2) and adenine at 1610 cm^{-1} (adenine N7) in the difference spectra of PEG-3350, PEG-6000, mPEG-anthracene, mPEG-PAMAM-G3, mPEG-PAMAM-G4 and PAMAM-G4 complexes of DNA (Figure 2, panels A & B, diffs, 1 mM). The observed intensity changes (particularly at high polymer content) were attributed to polymer interactions with DNA guanine N7, thymine O_2 and adenine N7 sites.[24,25] Similarly, increase in the intensity of the backbone PO_2 groups at 1225 (asymmetric PO_2) and 1088 cm^{-1} (symmetric PO_2 vibrations) were observed due to synthetic polymer-PO_2 interaction (Figure 2, panels A&B, diff., 1 mM).

The role of hydrophilic and hydrophobic contacts in polymer-DNA adducts

The shifting of the OH stretching of the free PEG at about 3430 cm^{-1} to a lower frequency in the infrared spectra of PEG-DNA complexes was attributed to the hydrophilic interaction between PEG and DNA polar groups. Similarly, the shifting of the NH stretching vibration at 3280 cm^{-1} in the spectra of the free dendrimer and pegylated dendrimerrs was due to the hydrophilic contacts between dendrimer terminal NH_2 groups and the DNA polar groups.[24,25] However, hydrophobic interactions between DNA and synthetic polymer were characterized by the shifting of the polymer antisymmetric and symmetric CH_2 stretching vibrations, in the region of 3000-2800 cm^{-1}. The CH_2 bands of the free PEG at 3000, 2990, 2940 cm^{-1} exhibited a minor shifting, while the CH_2 vibrations related to mPEG-PAMAM-G3 located at 2946, 2884 and 2859 cm^{-1}; for free mPEG-PAMAM-G4 at 2942, 2876 and 2856 cm^{-1} and free PAMAM-G4 at 2969, 2940 and 2834 cm^{-1} shifted to higher frequencies in the spectra of dendrimer-DNA adducts. The shifting of the polymer antisymmetric and symmetric CH_2 stretching vibrations in the region 3000-2800 cm^{-1} of the infrared spectra suggests the presence of hydrophobic interactions *via* dendrimer hydrophobic cavities and DNA hydrophobic groups.[24,25]

Conformation of DNA in polymer complexes

The CD spectrum of the free DNA is composed of four major peaks at 211 (negative), 220 (positive), 245 (negative) and 275 nm (positive) (Figure 3). This is consistent with CD spectra of double helical DNA in B conformation.[32,33] As polymer-DNA complexes formed, a major increase in molar ellipticity of the band at 210 nm occurred and the amplitude of the band at 245 was reduced, while the intensity of the band at 275 decreased at high polymer concentration (Figure 3, panel A). However, no major shifting was observed for the band at 275 nm in the spectra of polymer-DNA complexes (Figure 3, panels A & B). This is due to the presence of DNA in B-conformation both in the free state and in the synthetic polymer-DNA adducts. This is also consistent with the infrared results that showed free DNA in B-conformation with IR marker bands at 1710 (G), 1225 (PO_2), 892 and 834 cm^{-1} (ribose-phosphate) with no major shifting of these bands in the polymer-DNA complexes (Figure 2, panels A & B).

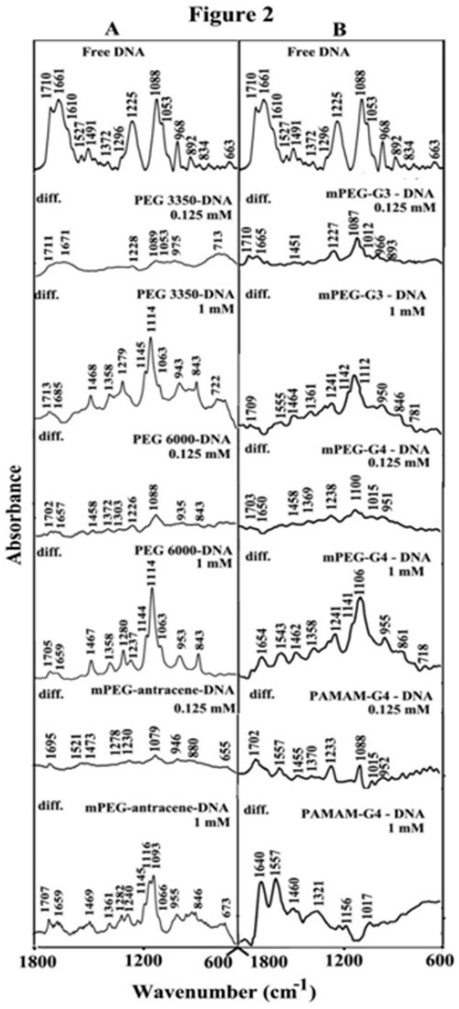

Figure 2 FTIR spectra and difference spectra [(DNA solution + polymer solution) -(DNA solution)] in the region of 1800-600 cm^{-1} for the free DNA and its synthetic polymer complexes with PEG-3350, PEG-6000 and mPEG-anthracene (panel A) and for mPEG-PAMAM-G3, mPEG-PAMAM-G4 and PAMAM-G4 (panel B) in aqueous solution at pH 7.3 with various polymer concentrations (0. 125 and 1 mM) and constant tRNA content (12.5 mM).

The reduced intensity of the band at 275 nm, in the spectra of polymer-DNA complexes together with the major intensity changes of the band at 210 and 220 nm were attributed to the condensation and particle formation of DNA, in the presence of PEG-3350, PEG-6000, mPEG-anthracene (Figure 3, panel A) and mPEG-PAMAM-G3, mPEG-PAMAM-G4 and particularly in PAMAM-G4-DNA adducts (Figure 3, panel B). The extent of decrease of intensity was much pronounced in the case of PAMAM-G4 nanoparticles, where DNA condensation, compaction and particle formation were observed (Figure 3, panel B). This is consistent with AFM images of the synthetic polymer-DNA complexes that showed major DNA condensation and particle formation by PAMAM-G4 nanoparticles (Figure 1, panel B).

Citation: Froehlich E, Mandeville JS, Bekale L, et al. DNA compaction and particle formation by synthetic polymers: applications in gene delivery. *J Nanomed Res.* 2015;2(4):117–122. DOI: 10.15406/jnmr.2015.02.00038

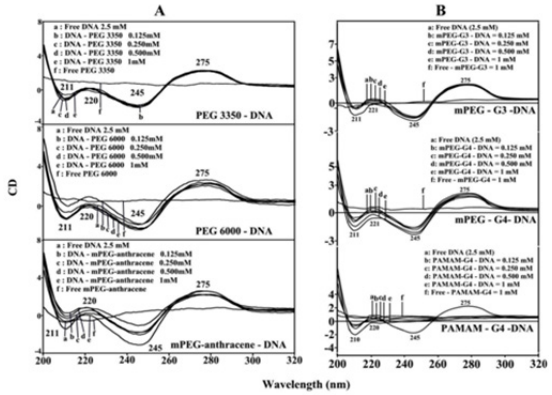

Figure 3 CD spectra of DNA in Tris-HCl (pH ~ 7.3) at 25 °C (2.5 mM) with PEG-3350, PEG-6000 and mPEG-anthracene (panel A) and mPEG-PAMAM-G3, mPEG-PAMAM-G4 and PAMAM-G4 (panel B) with 0.125, 0.25, 0.5 and 1 mM polymer concentrations.

Stability of polymer-DNA adducts

A comparison of the stability of synthetic polymer-DNA adducts by UV-visible spectroscopy .[34] showed $K_{PEG\ 3350\text{-}tRNA}$= 7.9 x 10^3 M^{-1}, $K_{PEG\ 6000\text{-}tRNA}$ = 1.5 x 10^4 M^{-1} and $K_{mPEG\text{-}anthracene}$= 3.6 x 10^3 M^{-1} , $K_{mPEG\text{-}G3}$= 1.5 x 10^3 M^{-1}, $K_{mPEG\text{-}G4}$= 3.4 x 10^3 M^{-1} and $K_{PAMAM\text{-}G4}$= 8.2 x 104 M^{-1} (Figure 4, panels A & B) .[23,24] Stronger polymer-DNA complexation formed by PEG-6000 than PEG-3350 and mPEG-anthracene, while PAMAM-G4 forms more stable complexes with DNA than those of PEGylated dendrimers with the order of binding PAMAM-G4>PEG-6000>PEG-3350>mPEG-anthracene>mPEG-PAMAM-G4>mPEG-PAMAM-G3 (Figure 4, panels A & B).[24,25] This is indicative of PEG forms stronger complexes than mPEG and PEGylated dendrimers. Similarly, stronger complexes form with larger PEG than smaller PEG. This is also consistent with the conclusion that synthetic polymer-DNA interaction is more hydrophilic than hydrophobic. This conclusion can be supported by the argue that PEG with mostly hydrophilic character forms stronger complexes with DNA, while mPEG-anthracene, with mostly hydrophobic nature forms weaker DNA complexes. Similarly, PAMAM-G4 which has more cationic NH_2 groups (64 NH_2 groups) than those of mPEG-PAMAM-G4 (32 NH_2 groups) and mPEG-PAMAM-G-3 (8 NH_2 groups) forms stronger complexes than PEGylated dendrimers (Figure 4, panels A & B).[24,25] The results showed that hydrophilic interaction is a major part of synthetic-polymer-DNA complexation.

The number of binding sites occupied by polymer on DNA duplex

Since DNA is a weak fluorophore, the titration of mPEG-anthracene was done against various DNA concentrations, using mPEG-anthracene excitation at 330-350 nm and emission at 400-450 nm.[35,36] When mPEG-anthracene interacts with DNA, fluorescence may change depending on the impact of such interaction on the mPEG-anthracene conformation or via direct quenching effect.[37] The decrease of fluorescence intensity of mPEG-anthracene has been monitored at 420 nm for mPEG-anthracence-DNA systems. The plot of F_0 / (F_0 – F) vs 1 / [DNA] is shown in Figure 5A. Assuming that the observed changes in fluorescence come from the interaction between mPEG-anthracene and polynucleotides, the quenching constant can be taken as the binding constant of the complex formation. The binding constant obtained was $K_{mPEG\text{-}anthracene\text{-}DNA}$ = 8.2 x 10^3 M^{-1} (Figue 5A'). The association constant calculated for the mPEG-anthracene-DNA adduct suggests low affinity mPEG-anthracene-DNA, which is consistent with the UV results discussed above. The *f* values obtained in Figure 5, suggest that DNA also interacts with fluorophore via hydrophobic interactions, which is consistent with our infrared spectroscopic results discussed (hydrophilic and hydrophobic contacts).

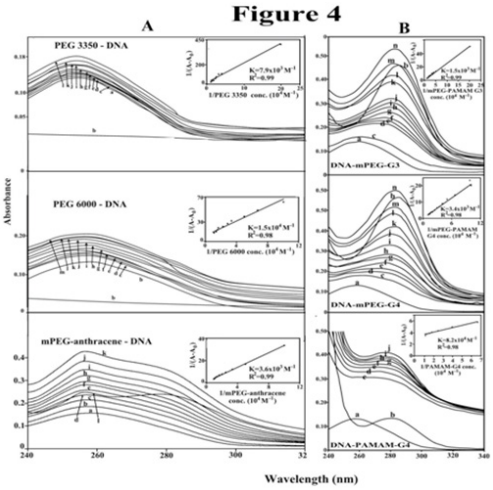

Figure 4 UV-visible results of DNA and its PEG-3350, PEG-6000 (B) and mPEG-anthracene complexes (panel A) and for mPEG-PAMAM-G3, mPEG-PAMAM-G4 and μM PAMAM-G4 complexes (panel B) with free DNA (100 μM); b) free polymer (100); titrated with polymer (5 to 80 μM). Plot of 1/(A-A0) vs (1/polymer concentration) for *K* calculation of polymer and DNA complexes, where A0 is the initial absorbance of DNA (260 nm) and A is the recorded absorbance (260 nm) at different polymer concentrations (5 μM to 100 μM) with constant DNA concentration of 100 μM at pH 7.3.

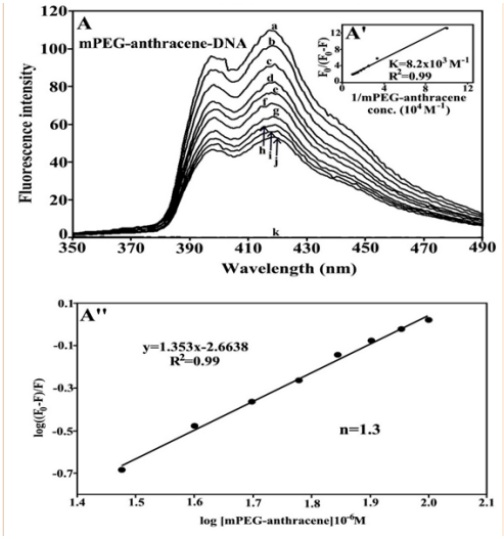

Figure 5 Fluorescence emission spectra of mPEG-anthracene-DNA systems in 10 mM Tris-HCl buffer pH 7.3 at 25 °C for A) polymer-DNA: (a) free mPEG-anthracene (80 μM), (b-j) with polymer-DNA complexes at 5 to 100 μM with (l) free DNA 100 μM. The plot of F0/(F0- F) as a function of 1/DNA concentration. The bindingconstant K being the ratio of the intercept and the slope for (A') mPEG-anthracene-DNA. The plot of log (F_0-F)/F as a function of log [DNA] for calculation of number of binding sites occupied by mPEG-anthracene molecules on DNA (n) in polymer-DNA adducts (A").

The number of binding sites occupied by mPEG-anthracene molecule on DNA (*n*) was calculated from log [(F_0 -F)/F] = logK_S + *n* log [DNA] for the static quenching.[38-41] The linear plot of log [(F_0-F]/F] as a function of log [DNA] is shown in Figure 5A". The *n* values from the slope of the straight line was 1.3 for mPEG-

Citation: Froehlich E, Mandeville JS, Bekale L, et al. DNA compaction and particle formation by synthetic polymers: applications in gene delivery. *J Nanomed Res.* 2015;2(4):117–122. DOI: 10.15406/jnmr.2015.02.00038

anthracene-DNA adduct (Figure 5A"). It seems that about one binding site is occupied by the PEG and mPEG-anthracene on DNA in these polymer-DNA adducts.

Conclusion

Spectroscopic and AFM data of the bindings of several synthetic polymers with DNA were compared here and the following points are concluded. a) Synthetic polymers bind DNA through a major hydrophilic interaction and a minor hydrophobic contact. b) The binding is mainly through polymer polar groups (OH, NH_2 and C-O) and DNA bases and the backbone-phosphate group. c) The order of binding is PAMAM-G4>PEG-6000>PEG-3350>mPEG-anthracene>mPEG-PAMAM-G4>mPEG-PAMAM-G3. d) Synthetic polymer complexation induces major DNA condensation, compaction and particle formation, while biopolymer remains in B-family structure. e) This study shows that synthetic polymers have profound effect on DNA morphology that can be of a major importance in gene delivery and DNA transfection. However, major differences were observed between synthetic polymer-DNA complexes and those of the polymer-RNA adducts.[42]

Acknowledgments

None.

Conflicts of interest

None.

References

1. Zhao Z, Chen T, Wang L et al. Nanotechnology in therapeutics: a focus on nanoparticles as a drug delivery system. *Nanomedicine.* 2012;7(8):1253–1271.
2. Davis ME, Chen ZG, Shin DM Nanoparticle therapeutics: an emerging treatment modality for cancer. *Nat Rev Drug Discovery.* 2008;7(9):771–782.
3. Haag R, Kratz F Polymer therapeutics: Concepts and applications. *Angew Chem Int Ed.* 2006;45(8):1198–1215.
4. Knop K, Hoogenboom R, Fischer D et al. Poly(ethylene glycol) in drug delivery: pros and cons as well as potential alternatives. *Angew Chem Int Ed.* 2010;49(36):6288– 6308.
5. Kavitha K, BhalaMurugan GL A review on PEGylation in anti–cancer drug delivery systems. *Int J Res Pharm Biomed Sci.* 2013;4(1):296–304.
6. Cao Z, Jiang S Super–hydrophilic zwitterionic poly(carboxybetaine) and amphihilicnon–ionic poly(ethylene glycol) for stealth nanoparticles. *Nano Today.* 2014;7(5):404–413.
7. Li A, Lehmann HP, Sun G et al. Synthesis and in vivo pharmacokinetic evaluation of degradable shell cross– linked polymer nanoparticles with poly(carboxybetaine) versus poly–(ethylene glycol) surface–grafted coatings. *ACS Nano.* 2012;6(10):8970–8982.
8. Maiti PK, Caing T, Wang G et al. Structure of PAMAM dendrimers: Generations 1 through 11. *Macromolecules.* 2004;37(16):6236–6254.
9. Samal SK, Dash M, Vlierberghe SV et al. Cationic polymers and their therapeutic potential. *Chem Soc Rev.* 2012;41(21):7147–7194.
10. Duncan R, Izzo L Dendrimer biocompatibility and toxicity. *Adv Drug Deliv Rev.* 2005;57(15):2215–2237.
11. Stiriba SE, Frey H, Haag R Dendritic polymers in biomedical applications: From potential to clinical use in diagnostics and therapy. *Angew Chem Int Ed.* 2002;41(8):1329–1334.
12. Di Gioia S, Conese M Polyethylenimine–mediated gene delivery to the lung and therapeutic applications. *Drug Design Develop Ther.* 2008;2:163–188.
13. Alexander TF Dendrimers: a versatile targeting platform. *Adv Drug Deliv Rev.* 2005;57(15):2104–2105.
14. Wolinsky JB, Grinstaff MW Therapeutic and diagnostic applications of dendrimers for cancer treatment. *Adv Drug Deliv Rev.* 2008;60(9):1037–1055.
15. Yuan Q, Yeudall WA, Yang H PEGylated polyamidoamine dendrimers with bis–aryl hydrazone linkages for enhanced gene delivery. *Biomacromolecules.* 2010;11(8):1940–1947.
16. Kojima C, Kono K, Maruyama K et al. Synthesis of Polyamidoamine Dendriemrs having poly(ethylene glycol) grafts and their Ability to encapsulate anticancer drugs. *Bioconjug Chem.* 2008;11(6):910–917.
17. Fant K, Esbjorner EK, Jenkins A et al. Effects of PEGylation and acetylation of PAMAM dendrimers on DNA binding, cytotoxicity and in vitro transfection efficiency. *Mol Pharm.* 2010;7(5):1743–1746.
18. Bello–Roufai M, Lambert O, Pitard B Relationships between the physicochemical properties of an amphiphilic triblock copolymers/ DNAcomplexes and their intramuscular transfection efficiency. *Nucl Acids Res.* 2007;35(3):728–739.
19. Wang R, Zhou L, ZhouY et al. Synthesis and gene delivery of poly(amido amines) with different branched architecture. *Biomacromolecules.* 2010;11(2):489–495.
20. Patri AK, Majoros IJ, Baker JR Dendritic polymer macromolecularcarriers for drug delivery. *Curr Opinion Chem Biol.* 2002;6(4):466–471.
21. Evans HM, Ahmad A, Ewert K et al. Structural polymorphism of DNA–dendrimer complexes. *Phys Rev Lett.* 2003;91(7):075501.
22. Nandy B, Maiti PK DNA compaction by a dendrimer. *J Phys Chem B.* 2011;115(2):217–230.
23. Ottaviani MF, Furini F, Casini A et al. Formation of supramolecular structures between DNA and starburst dendrimers studied by EPR, CD, UV, and melting profiles. *Macromolecules*. 2000;33(21):7842–7851.
24. Froehlich E, Mandeville JS, Weinert CM et al. Bundling and aggregation of DNA by cationic dendrimers. *Biomacromolecules.* 2011;12(2):511–517.
25. Froehlich E, Mandeville JS, Arnold D et al. PEG and mPEG–anthracene induce DNA condensation and particle formation. *J Phys Chem B.* 2011;115(32):9873–9879.
26. Marty R, N'soukpoe–Kossi CN, Charbonneau D et al. Structural Analysis of DNA complexation with cationic lipids. *Nuclelic Acids Res.* 2009;37(3):849–857.
27. Alex S, Dupuis P FTIR and Raman investigation of cadmium binding by DNA. *Inorg Chim Acta.* 1989;157(2):271–281.
28. Andrushchenko VV, Leonenko Z, van de Sande H et al. Vibrational CD (VCD) and atomic force microscopy (AMF) study of DNA interactions with Cr3+: VCD and AFM evidence of DNA condensation. *Biopolymers.* 2002;61:243–260.
29. Dovbeshko GI, Chegel VI, Gridina NY et al. Surface enhanced IR absorption of nucleic acids from tumor cells: FTIR reflectance study. *Biopolymers.* 2002;67(6):470–486.
30. Ouameur AA, Bourassa P, Tajmir–Riahi HA Probing tRNA interaction with biogenic polyamines. *RNA.* 2010;16(10):1968–1979.
31. Ouameur AA, Tajmir–Riahi HA Structural analysis of DNA interactions with biogenic polyamines and cobalt (III) hexamine studied by Fourier transform infrared and capillary electrophoresis. *J Biol Chem.* 2004;279(40):42041–42054.

32. Kypr J, Vorlickova M Circular dichroism spectroscopy reveal invariant conformation of guanine runs in DNA. *Biopolymers.* 2002;67(4–5):275–277.

33. Vorlickova M Conformational transitions of alternating purine–pyrimidine DNAs in the perchlorate ethanol solutions. *Biophys J.* 1995;69(5): 2033–2043.

34. Connors K Binding constants: The measurement of molecular complex Stability. *John Wiley & Sons, New York, USA.* 1987

35. del Valle JC, Turek AM, Tarkalanov ND, Saltiel J Distortion of the fluorescence spectrum of anthracene with increasing laser puls excitation energy. *J Phys Chem A.* 2002;106(20):5101–5104.

36. Zheng Y, Micic M, Mello SV, Mabrouki M, Andreopoulos FM, et al. PEG–based hydrogel synthesis via the Photodimerization of anthracene groups. *Macromolecules.* 2002;35(13):5228–5234.

37. Lakowicz JR In Principles of Fluorescence Spectroscopy. *(3rd edn), Springer, New York, USA.* 2006

38. Froehlich E, Mandeville JS, Weinert CM et al. Aggregation and particle formation of tRNA by dendrimers. *Biomacromolecules.* 2011;12(7):2780–2787.

39. Froehlich E, Mandeville JS, Arnold D et al. The effect of PEG and mPEG–anthracene on tRNA aggregation and particle formation. *Biomacromolecules.* 2012;13(1):282–287.

40. Sanyakamdhorn S, Chanphai P, Tajmir–Riahi HA Encapsulation of biogenic and synthetic polyamines by nanoparticles PEG and mPEG–anthracene. *J Photochem Photobiol B.* 2014;130:30–39.

41. Mandeville JS, N'soukpoé–Kossi CN, Neault JF, Tajmir–Riahi H A Structural analysis of DNA interaction with retinol and retinoic acid. *Biochem Cell Biol.* 2010;88(3):469–477.

42. Tajmir–Riahi HA, Bekale L, Kreplak L Effect of synthetic polymers on tRNA nanoparticle formation. *J Nanomed Res.* 2015;2(3):00031.

Citation: Froehlich E, Mandeville JS, Bekale L, et al. DNA compaction and particle formation by synthetic polymers: applications in gene delivery. *J Nanomed Res.* 2015;2(4):117–122. DOI: 10.15406/jnmr.2015.02.00038